J|A|C|S
ARTICLES
Published on Web 06/25/2004

Synthesis and Properties of Compressed Dihydride Complexes of Iridium: Theoretical and Spectroscopic Investigations

Ricard Gelabert, Miquel Moreno, José M. Lluch,* Agustí Lledós,* Vincent Pons, and D. Michael Heinekey*

Contribution from the Departament de Química, Universitat Autònoma de Barcelona, 08193 Bellaterra, Barcelona, Spain, and Department of Chemistry, University of Washington, Seattle, Washington 98195-1700

Received March 3, 2004; E-mail: lluch@klingon.uab.es

Abstract: Reaction of $[Cp^*Ir(P-P)Cl][B(C_6F_5)_4]$ (P−P = bisdimethydiphosphinomethane (dmpm), bisdiphenyldiphosphinomethane (dppm)) with $[Et_3Si][B(C_6F_5)_4]$ in methylene chloride under 1 atm of hydrogen gas affords the dicationic compressed dihydride complexes $[Cp^*Ir(P-P)H_2][B(C_6F_5)_4]_2$. These dicationic complexes are highly acidic and are very readily deprotonated to the corresponding monohydride cations. When the preparative reaction is carried out under HD gas, the hydride resonance exhibits $J_{HD} = 7-9$ Hz, depending upon the temperature of observation, with higher values of J_{HD} observed at higher temperatures. A thermally labile rhodium analogue, $[Cp^*Rh(dmpm)(H_2)][B(C_6F_5)_4]_2$, was prepared similarly. A sample prepared with HD gas gave $J_{HD} = 31$ Hz and $J_{HRh} = 31$ Hz, allowing the Rh complex to be identified as a dihydrogen complex. Quantum dynamics calculations on a density functional theory (DFT) potential energy surface have been used to explore the structure of the Ir complexes, with particular emphasis on the nature of the potential energy surface governing the interaction between the two hydride ligands and the Ir center.

1. Introduction

Transition metal dihydrogen complexes have emerged as a fascinating area of research in coordination chemistry. Early work in this area focused on dihydrogen complexes with a largely intact hydrogen molecule coordinated to the metal center ($R_{HH} < 1.0$ Å).[1] Subsequently, a modest number of complexes have been reported which have longer H−H distances up to *ca.* 1.4 Å. Such complexes have been termed elongated dihydrogen complexes and are of particular interest in that they may represent an arrested intermediate state in the very important oxidative addition reaction.[2] Fascinating properties have been reported for some of these molecules. Particularly interesting are a family of Ru complexes exemplified by $[Cp^*Ru(dppm)H_2]^+$ (dppm = bisdiphenylphosphinomethane), where $R_{HH} = 1.10$ Å has been established by neutron diffraction.[3] A theoretical study of this complex using density functional theory (DFT) calculations showed that the two hydrogen atoms are bound in a soft and highly anharmonic potential energy surface (PES). This study led to the intriguing prediction that R_{HH} in this complex will increase slightly with temperature, due to population of low-lying vibrational excited states and that the bond distance will be sensitive to isotopic substitution, with the distance in the H−H complex predicted to be approximately 10% longer than in the corresponding T−T complex.[4] These predictions were subsequently verified by experiment.[5] These experiments rely on the well-established inverse correlation between H−D coupling and H−H distance R_{HH}.[6−8] Thus, the observed values of J_{HD} in partially deuterated samples of the Ru complex decrease with increasing temperature, signaling that the thermally averaged value of R_{HH} is increasing.

We now report the preparation of dicationic Rh and Ir analogues of these ruthenium complexes. The preparation of these complexes required the development of new synthetic methodologies for halide abstraction from positively charged precursors. For Rh, an elongated dihydrogen complex is observed. In the case of Ir, the resulting dicationic complexes are best described as compressed dihydride complexes, based on T_1 and J_{HD} data. In contrast to the previous studies of cationic Ru complexes, the observed value of J_{HD} increases with increasing observation temperature. An improved procedure has been developed for the correlation of R_{HH} with J_{HD} for

(1) General reviews: (a) Kubas, G. J. *Metal Dihydrogen and σ-Bond Complexes: Structure, Theory and Reactivity*. Kluwer: New York, 2001. (b) Heinekey, D. M.; Oldham, W. J., Jr. *Chem. Rev.* **1993**, *93*, 913. (c) Morris, R. H.; Jessop, P. G. *Coord. Chem. Rev.* **1992**, *121*, 155. (d) McGrady, G. S.; Guilera, G. *Chem. Soc. Rev.* **2003**, *32*, 383.
(2) Heinekey, D. M.; Lledós, A.; Lluch, J. M. *Chem. Soc. Rev.* **2004**, *33*, 175.
(3) Klooster, W. T.; Koetzle, T. F.; Jia, G.; Fong, T. P.; Morris, R. H.; Albinati, A. *J. Am. Chem. Soc.* **1994**, *116*, 7677.
(4) Gelabert, R.; Moreno, M.; Lluch, J. M.; Lledós, A. *J. Am. Chem. Soc.* **1997**, *119*, 9840.
(5) Law, J. K.; Mellows, H.; Heinekey, D. M. *J. Am. Chem. Soc.* **2002**, *124*, 1024.
(6) Heinekey, D. M.; Luther, T. A. *Inorg. Chem.* **1996**, *35*, 4396.
(7) Maltby, P. A.; Schlaf, M.; Steinbeck, M.; Lough, A. J.; Morris, R. H.; Klooster, W. T.; Koetzle, T. F.; Srivastava, R. C. *J. Am. Chem. Soc.* **1996**, *118*, 5396.
(8) Gründemann, S.; Limbach, H. H.; Buntkowsky, G.; Sabo-Etienne, S.; Chaudret, B. *J. Phys. Chem. A* **1999**, *103*, 4752.

complexes of this type, which has eliminated a previously reported discrepancy between relaxation and coupling data.

Calculations of the electronic structure of complex [Cp*Ir(dmpm)H_2]$^{2+}$ ($\mathbf{1}^{2+}$) (dmpm = bisdimethylphosphinomethane) have been carried out in combination with a nuclear dynamics study. The structure of $\mathbf{1}^{2+}$ deduced from these studies is consistent with the experimental observation. The calculated potential energy surface for the interaction of the two hydride ligands with the Ir center leads to an understanding of the temperature dependence of the observed HD coupling constant in **1**-d_1.

A portion of the results described here has been previously communicated.[9]

2. Experimental Details

2.1. General Procedures. Unless stated otherwise, all manipulations were carried out under argon using Schlenk techniques. Phosphine ligands were obtained from Strem Chemicals and used as received. Hydrogen gas was purchased from Airgas and passed through a column of activated molecular sieves prior to use. HD (g) and D_2 (g) were used as received from Cambridge Isotopes. Elemental analyses were performed by Galbraith. NMR spectra were recorded on Bruker AC-200, DPX-200, DRX-499, AM-500, and DMX-750 spectrometers. Proton NMR spectra were referenced to the solvent resonance with chemical shifts reported relative to TMS. ^{31}P chemical shifts were referenced to external 85% H_3PO_4. The NMR studies were carried out in high quality 5 mm NMR tubes, utilizing deuterated solvent distilled from standard drying agents. The conventional inversion−recovery method (180-τ-90) was used to determine the relaxation times T_1. In each experiment the waiting period was longer than 10 times the expected relaxation rate. Ten variable delays were employed, utilizing appropriate pulse widths. Workup of spectra used for precise measuring of coupling constants used zero filling to 128K data points prior to Fourier transform.

2.2. Synthesis. [Cp*Ir(dmpm)Cl]Cl. The ligand dmpm (55 μL, 0.348 mmol) was added to a solution of 70 mg (0.175 mmol) of $[Cp^*IrCl_2]_2$ in 30 mL of degassed methanol. After the solution was stirred for 2 h under reflux, it was concentrated to approximately 5 mL, and the product precipitated by addition of 5 mL of Et_2O. Recrystallization in CH_2Cl_2/Et_2O (50/50) at −26 °C affords 160 mg [Cp*IrdmpmCl]Cl·$2H_2O$ (78%). Anal. calcd for $C_{15}H_{29}Cl_2IrP_2\cdot 2H_2O$: C, 31.58; H, 5.83. Found: C, 31.65; 5.89 H. ^{1}H NMR δ ($CDCl_3$, 500 MHz) 6.14 (m, 1 H, CH), 3.49 (m, 1 H, CH), 1.95 (t, $^4J_{P-H}$ = 2.5 Hz, 15 H, $C_5(CH_3)_5$) 2.19, 1.77 ("t", $^2J_{P-H}$ = 6 Hz, 3 H, $P(CH_3)_2$). ^{31}P{^{1}H} δ ($CDCl_3$, 202.34 MHz) −59.4 (s). The previously reported complexes $[Cp^*Ir(dppm)Cl]^+$ and $[Cp^*Rh(dmpm)Cl]^+$ were prepared similarly.

[Cp*Ir(dppm)Cl]Cl. ^{1}H NMR, δ, ($CDCl_3$, 500 MHz) 7.57, 7.49, 7.27 (m, 20 H, $P(C_6H_5)_2$), 6.57 (d of t, $^2J_{H-H}$ = 15.5 Hz, $^2J_{H-P}$ = 9.5 Hz, 1 H, CH), 4.67 (d of t, $^2J_{H-H}$ = 15.5 Hz, $^2J_{H-P}$ = 13 Hz, 1 H, CH), 1.80 (t, $^4J_{P-H}$ = 2.5 Hz, 15 H, $C_5(CH_3)_5$). ^{31}P{^{1}H} δ ($CDCl_3$, 202.34 MHz) −37.1 (s).

[Cp*Rh(dmpm)Cl]Cl. ^{1}H NMR, δ, ($CDCl_3$, 499.85 MHz) 4.8 (d of t, $^2J_{H-H}$ = 14 Hz, $^2J_{H-P}$ = 11 Hz, 1 H, CH), 3.39 (d of t, $^2J_{H-H}$ = 14 Hz, $^2J_{H-P}$ = 13.5 Hz, 1 H, CH), 1.88 (t, $^4J_{P-H}$ = 3.5 Hz, 15 H, $C_5(CH_3)_5$), 2.13, 1.77 ("t", $^2J_{P-H}$ = 6 Hz, 3 H, $P(CH_3)_2$). ^{31}P{^{1}H} δ ($CDCl_3$, 202.34 MHz) −22.09 (d, $^1J_{Rh-P}$ = 109 Hz).

[Cp*Ir(dmpm)H_2][$B(C_6F_5)_4$]$_2$ (1). In a typical experiment, an NMR tube fitted with a high vacuum Kontes valve was charged with 40 mg of $Ph_3CB(C_6F_5)_4$. Et_3SiH (1 to 2 mL) was added by vacuum transfer. After the yellow−orange mixture was stirred overnight, excess Et_3SiH was removed by pumping, and 10 mg of [Cp*Ir(dmpm)Cl]Cl was added. CD_2Cl_2 was added by vacuum transfer, and the tube was degassed and flame sealed under 1 atm of H_2 (or HD). ^{1}H NMR δ (CD_2Cl_2, 499.85 MHz, 240 K) 5.01 (m, 1 H, CH), 3.70 (m, 1 H, CH), 2.28 (t, $^3J_{H-P}$ = 2 Hz, 15 H, $C_5(CH_3)_5$ of *cis*-IrH_2), 2.20, 2.01 (m, 6 H, $P(CH_3)_2$ of *cis*-IrH_2), 2.39 (br. s, 15 H, $C_5(CH_3)_5$ of *trans*-IrH_2), 2.25, 2.17 (br. s, 6 H, $P(CH_3)_2$ of *trans*-IrH_2), −10.53 (t, $^2J_{H-P}$ = 6 Hz, *cis*-IrH_2), −10.60 (t, $^2J_{H-P}$ = 20 Hz,. *trans*-IrH_2). ^{31}P{^{1}H} δ (CD_2Cl_2, 202 MHz, 240 K) −76.2 (s).

The Ir complex **2** and the Rh complex [Cp*Rh(dmpm)(H_2)][$B(C_6F_5)_4$]$_2$ were prepared similarly.

[Cp*Ir(dppm)H_2][$B(C_6F_5)_4$]$_2$ (2). ^{1}H NMR, δ (CD_2Cl_2, 750.13 MHz, 300 K) 8−7.4 (m, 20 H, $P(C_6H_5)_2$, 5.82 (m, 1 H, CH), 4.2 (m, 1 H, CH), 1.75 (s (broad), 15 H, $C_5(CH_3)_5$, *cis*-IrH_2), 2.17 (s (broad), 15 H, $C_5(CH_3)_5$, *trans*-IrH_2), −9.31 (s (broad), 2 H, *cis*-IrH_2), −9.50 (t, $^2J_{H-P}$ = 17 Hz, 2 H, *trans*-IrH_2).^{31}P sel. {^{1}H} δ (CD_2Cl_2, 303.65 MHz, 300 K) −23.42 (t, *trans*-IrH_2, $^2J_{H-P}$ = 17 Hz), −54.73 (s (broad), *cis*-IrH_2).

[Cp*Rh(dmpm)(HD)][$B(C_6F_5)_4$]$_2$. ^{1}H {^{31}P} NMR, δ (CD_2Cl_2, 750.13 MHz) 5.5 (m, 1 H, CH), 3.9 (m, 1 H, CH), 2.12 (s, 15 H, $C_5(CH_3)_5$), 1.97, 1.94 (s, 3 H, $P(CH_3)_2$), −3.61 (d of t, $^1J_{Rh-H}$ = 31 Hz, $^1J_{H-D}$ = 31 Hz, 1 H, Rh(HD)).

[Cp*Ir(dppm)H][$B(C_6F_5)_4$]. ^{1}H NMR, δ (CD_2Cl_2, 750 MHz) 7.57, 7.52, 7.34 (m, 20 H, $P(C_6H_5)_2$, 5.88 (d of t, $^2J_{H-H}$ = 16 Hz, $^2J_{H-P}$ = 10 Hz, 1 H, CH), 4.23 (d of t, $^2J_{H-H}$ = 16 Hz, $^2J_{H-P}$ = 12 Hz, 1 H, CH), 1.89 (b s, 15 H, $C_5(CH_3)_5$), −14.35 (t, $^2J_{H-P}$ = 25 Hz, 1 H, IrH). ^{31}P sel {^{1}H} δ (CD_2Cl_2, 303.65 MHz, 300 K) −40.08 (d, $^2J_{H-P}$ = 25 Hz).

[Cp*Ir(dmpm)H][$B(C_6F_5)_4$]. ^{1}H NMR, δ (CD_2Cl_2, 200 MHz) 5.01 (m, 1H, CH), 3.58 (m, 1H, CH), 2.27 (t, $^4J_{H-P}$ = 2.5 Hz, 15 H, $C_5(CH_3)_5$), 2.15, 1.91 (m, 6 H each, $P(CH_3)_3$), −15.09 (t, $^2J_{H-P}$ = 25 Hz, 1 H, IrH). ^{31}P sel. {^{1}H} δ (CD_2Cl_2, 303.65 MHz, 300 K) −68.6 (d, $^2J_{H-P}$ = 25 Hz).

[Cp*Ir(dmpm)Cl][$B(C_6F_5)_4$]. A vial was charged with 170 mg of $(Ph_3)CB(C_6F_5)_4$ (0.184 mmol), 84 mg of [Cp*Ir(dmpm)Cl]Cl (0.155 mmol), and 5 mL of methylene chloride. After the solution was stirred for 1 h, the solvent was evaporated, and the remaining solid was washed with 4 × 5 mL ether. Crystals were obtained by slow diffusion of Et_2O into a solution of [Cp*Ir(dmpm)Cl][$B(C_6F_5)_4$] in CH_2Cl_2. The anion exchange was monitored by ^{1}H NMR spectroscopy, since the resonances due to the protons of the CH_2 and PMe_2 groups are very sensitive to a change of anion. 184 mg of [Cp*Ir(dmpm)Cl][$B(C_6F_5)_4$] was recovered, 100% yield. ^{1}H NMR δ ($CDCl_3$, 499.85 MHz) 4.76 (m, 1 H, CH), 3.49 (m, 1 H, CH), 1.92 (t, $^4J_{P-H}$ = 2.5 Hz, 15 H, $C_5(CH_3)_5$), 1.80, 1.74 ("t", $^2J_{P-H}$ = 6 Hz, 3 H, $P(CH_3)_2$). ^{31}P{^{1}H} δ ($CDCl_3$, 202.34 MHz) −58.5 (s).

2.3. X-ray Structure of [Cp*Ir(dmpm)Cl][$B(C_6F_5)_4$]. Yellow crystals suitable for X-ray diffraction were obtained by diffusion of Et_2O into a solution of [Cp*Ir(dmpm)Cl][$B(C_6F_5)_4$] in CH_2Cl_2 and mounted on glass capillaries in oil. Diffraction measurements were made on a crystal fragment of dimensions 0.24 × 0.24 × 0.19 mm in a nitrogen stream at 130 K on a Nonius Kappa CCD diffractometer using graphite-monochromated radiation (λ = 0.710 73 Å). Crystal-to-detector distance was 30 mm, and exposure time was 10 s per degree for all sets. The scan width was 2.0°. Data collection was 81.4% complete to 28.35° in θ. A total of 12 856 reflections were collected covering the indices h = −11 to 11, k = −11 to 15, and l = −19 to 19. A total of 8265 reflections were symmetry independent, and the R_{int} = 0.0761 indicated that the data were of average quality. Indexing and unit cell refinement indicated a triclinic P lattice. The space group was found to be $P\bar{1}$ (No. 2) with cell parameters a = 11.5620(4) Å, b = 12.2440(5) Å, c = 15.1400(8) Å, α = 74.2690(18)°, β = 80.1290(15)°, and γ = 84.017(4)°. The cell volume was 2028.71 (15) Å^3, and the calculated density was 1.928 g/cm^3, with Z = 2. The data were integrated and scaled using *hkl*-SCALEPACK. Solution by direct methods produced a complete heavy atom phasing model closely related to the proposed structure. All hydrogen atoms were placed using a riding model. All non-hydrogen atoms were refined anisotropically by full-matrix least squares. Tables of data collection, solution, and refinement details, crystal data, atomic coordinates, and anisotropic thermal parameters are included in the Supporting Information.

(9) Pons, V.; Heinekey, D. M. *J. Am. Chem. Soc.* **2003**, *125*, 8428.

3. Calculational Details

3.1. Electronic Structure Calculations. For complex $\mathbf{1}^{2+}$, a global C_s symmetry has been enforced throughout as the sole geometrical constraint. The complete set of electronic structure calculations have been performed with the GAUSSIAN 98 program.[10] The DFT formalism has been used with the three-parameter hybrid functional of Becke and the Lee, Yang, and Parr's correlation functional, more widely known as B3LYP.[11,12] An effective core operator has been used to replace the inner electrons of the iridium atom,[13] while its outer electrons were described with the basis set associated with the pseudopotential of Hay and Wadt with a standard double-ζ LANL2DZ contraction.[10,13] For the phosphorus atoms, the same pseudopotential and basis set were used, enlarged with *d* polarization functions.[14] The remainder of the atoms of the system were described with the standard split-valence 6-31G basis set,[15] except for the five carbon atoms in the cyclopentadienyl ring and the one between the phosphorus atoms, for which the 6-31G(d) basis set was used,[16] and for the hydrogen atoms directly bound to the iridium, for which the 6-31G(p) basis set was used instead.[17] Localization of stationary points was achieved through use of the Schlegel algorithm within a redundant internal coordinate system.[10,18]

3.2. Nuclear Dynamics Calculations. This work is concerned with the dynamics of the dihydrogen ligand in complex $\mathbf{1}^{2+}$. Because of the light masses of the atoms involved, a static study based on locating and characterizing stationary points is not enough and their quantum nature has to be taken into account explicitly. Within the adiabatic separation of nuclear and electronic motions (Born−Oppenheimer approximation), the stationary states of nuclear motion are obtained by solving the nuclear Schrödinger equation:

$$(\hat{T}_{\mathrm{nuc}} + U(\mathbf{R}))\Psi = E\Psi \qquad (1)$$

Here, **R** is a 3*N*-6 dimensional vector describing the arrangement of the nuclei, and $U(\mathbf{R})$ is the potential energy hypersurface, obtained by solving the electronic Schrödinger equation for each nuclear arrangement and adding to the electronic energy obtained in this way the internuclear repulsion energy for that arrangement of nuclei. $\hat{T}_{\mathrm{nuc}}$ is the nuclear kinetic energy operator. Solving eq 1 using the discrete variable representation (DVR) methodology of Colbert and Miller[19] yields the stationary states that describe internal molecular motion, or, in other words, the vibrational states of the molecule, as a set of energies and nuclear wave functions.

4. Results

4.1. Synthesis. The precursor chloride complexes [Cp*Ir(dmpm)Cl]Cl and [Cp*Ir(dppm)Cl]Cl have been prepared by reaction of 4 equiv of dmpm and dppm, respectively, with $[Cp^*IrCl_2]_2$ in refluxing methanol (dmpm = bisdimethylphosphinomethane). The Rh complex [Cp*Rh(dmpm)Cl]Cl was prepared similarly. Recrystallization from methylene chloride/diethyl ether affords these complexes in high purity and adequate yield.

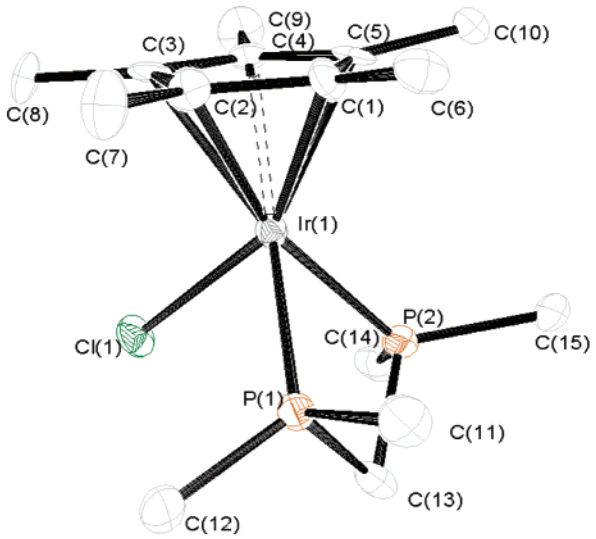

Figure 1. ORTEP drawing of the cationic portion of [Cp*Ir(dmpm)Cl]B(C_6F_5)$_4$. Hydrogen atoms have been omitted for clarity.

Table 1. Selected Bond Distances and Angles for [Cp*Ir(dmpm)Cl][B(C_6F_5)$_4$]

distances, Å		angles, deg	
Ir_1-Cl_1	2.3917(16)	$P_1-Ir_1-P_2$	71.81(6)
$Ir-P_1$	2.2989(18)	$P_1-C_{13}-P_2$	94.2 (4)
$Ir-P_2$	2.2904(18)	$Cp^*-Ir_1-P_1$	135.93
Ir−Cp* centroid	1.850	$Cp^*-Ir_1-P_2$	137.13
		$Cp^*-Ir_1-Cl_1$	123.13

Metathesis of [Cp*Ir(dmpm)Cl]Cl with $(Ph_3)CB(C_6F_5)_4$ affords [Cp*Ir(dmpm)Cl] B(C_6F_5)$_4$. Crystals suitable for X-ray diffraction were grown from methylene chloride/diethyl ether solutions. The structure of this complex is shown in Figure 1. Relevant bond distances and angles are listed in Table 1.

Reaction of [Cp*Rh(dmpm)Cl]Cl in methylene chloride under H_2 with 2 equiv of $[Et_3Si][B(C_6F_5)_4]$ affords a new thermally labile dicationic species. In addition to the expected resonances for the phosphine and Cp* ligands in the ^{1}H NMR spectrum, a very broad hydride resonance was detected at −3.55 ppm. When the preparative reaction was carried out under HD gas, the spectra shown in Figure 2 were obtained. The measured J_{HD} value is 31 Hz, which is approximately equal to J_{HRh}, leading to the observed four line pattern.

Reaction of [Cp*Ir(dmpm)Cl]Cl in methylene chloride with 2 equiv of $[Et_3Si][B(C_6F_5)_4]$ under H_2 affords $[Cp^*Ir(dmpm)H_2][B(C_6F_5)_4]_2$ (**1**). $[Et_3Si][B(C_6F_5)_4]$ was generated by reaction of Et_3SiH with $(Ph_3C)B(C_6F_5)_4$. A similar reaction with the dppm analogue gives $[Cp^*Ir(dppm)H_2][B(C_6F_5)_4]_2$ (**2**). Both **1** and **2** are characterized as mixtures of two isomeric dihydride species with both transoid and cisoid variants of a capped square pyramidal geometry (see Scheme 1).

In the case of **1**, the cis/trans ratio is 97:3; for complex **2**, the ratio is 65:35. The hydride resonance for the trans isomer exhibits much larger coupling to the adjacent ^{31}P nuclei in both

(10) Frisch, M. J.; Trucks, G. W.; Schlegel, H. B.; Scuseria, G. E.; Robb, M. A.; Cheeseman, J. R.; Zakrzewski, V. G.; Montgomery, J. A., Jr.; Stratmann, R. E.; Burant, J. C.; Dapprich, S.; Millam, J. M.; Daniels, A. D.; Kudin, K. N.; Strain, M. C.; Farkas, O.; Tomasi, J.; Barone, V.; Cossi, M.; Cammi, R.; Menucci, B.; Pomelli, C.; Adamo, C.; Clifford, S.; Ochterski, J.; Petersson, G. A.; Ayala, P. Y.; Cui, Q.; Morokuma, K.; Malick, D. K.; Rabuck, A. D.; Raghavachari, K.; Foresman, J. B.; Ciolowski, J.; Ortiz, J. V.; Baboul, A. G.; Stefanov, B. B.; Liu, G.; Liashenko, A.; Piskorz, P.; Komaroni, I.; Gomperts, R.; Martin, R. L.; Fox, D. J.; Keith, T.; Al-Laham, M. A.; Peng, C. Y.; Nanayakkara, A.; Challacombe, M.; Gill, P. M. W.; Johnson, B.; Chen, W.; Wong, M. W.; Andres, J. L.; Gonzalez, C.; Head-Gordon, M.; Replogle, E. S.; Pople, J. A. *Gaussian 98*, revision A.9; Gaussian, Inc.: Pittsburgh, PA, 1998.
(11) Lee, C.; Yang, W.; Parr, G. R. *Phys. Rev. B* **1988**, *37*, 785.
(12) Becke, A. D. *J. Chem. Phys* **1993**, *98*, 5648.
(13) Hay, P. J.; Wadt, W. R. *J. Chem. Phys.* **1985**, *82*, 299.
(14) Höllwarth, A.; Böhme, M.; Dapprich, S.; Ehlers, A. W.; Gobbi, A.; Jonas, V.; Köhler, K. F.; Stegmann, R.; Veldkamp, A.; Frenking, G. *Chem. Phys. Lett.* **1993**, *208*, 237.
(15) Hehre, W. J.; Ditchfield, R.; Pople, J. A. *J. Chem. Phys.* **1972**, *56*, 2257.
(16) Francl, M. M.; Pietro, W. J.; Hehre, W. J.; Binkley, J. S.; Gordon, M. S.; DeFrees, D. J.; Pople, A. A. *J. Chem. Phys.* **1982**, *77*, 3654.
(17) Hariharan, P. C.; Pople, J. A. *Theor. Chim. Acta* **1973**, *28*, 213.
(18) Peng, C.; Ayala, P. Y.; Schlegel, H. B.; Frisch, M. J. *J. Comput. Chem.* **1996**, *17*, 49.
(19) Colbert, D.; Miller, W. H. *J. Chem. Phys.* **1992**, *96*, 1982.

Scheme 1. Reaction of Ir Chloride Complexes with $[Et_3Si][B(C_6F_5)_4]$ under Hydrogen

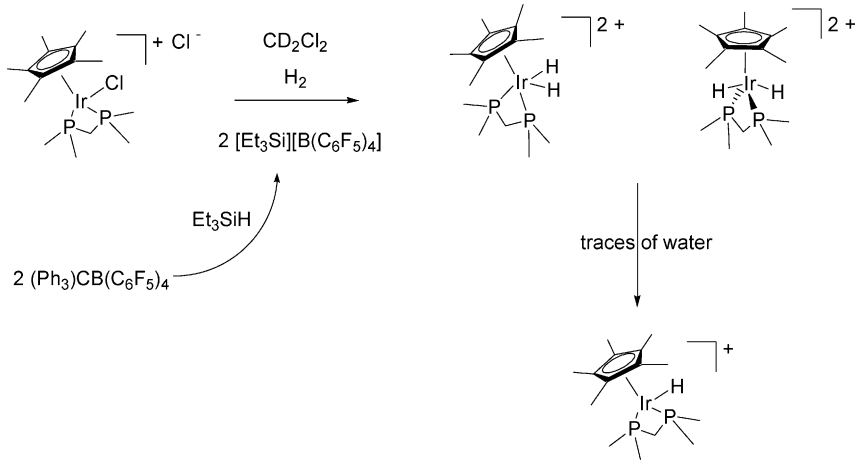

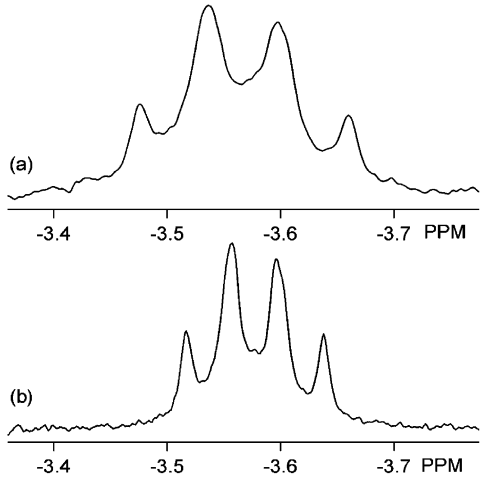

Figure 2. Partial $^1H\{^{31}P\}$ NMR spectrum of $[Cp^*Rh(dmpm)HD]^{2+}$ at (a) 500 MHz (CD_2Cl_2, 265 K) and (b) 750 MHz (CD_2Cl_2, 250 K).

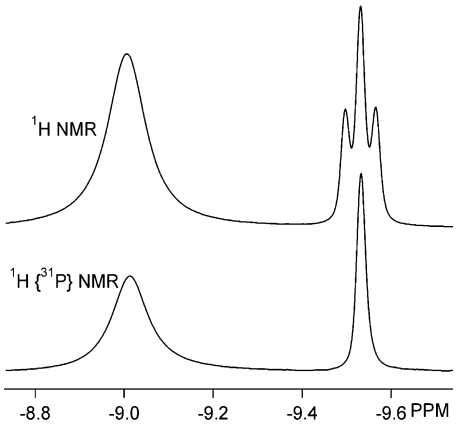

Figure 3. (Top) Partial (hydride region) ^1H NMR spectrum of $[Cp^*Ir(dppm)H_2][B(C_6F_5)_4]_2$ (**2**). (Bottom) $^1H\{^{31}P\}$ NMR spectrum (200 K, 500 MHz, CD_2Cl_2).

complexes. The signal due to the cis isomer is broad, due to rapid dipole−dipole relaxation (see below). The ^1H NMR spectrum of the hydride region for complex **2** is shown in Figure 3. While **1** and **2** are moderately stable thermally at ambient temperature (10% decomposition after 12 h), attempts to isolate these complexes were hampered by their very high acidity. Even in rigorously dried solvents, traces of water lead to deprotonation to the corresponding monohydride cations $[Cp^*Ir(dmpm)H][B(C_6F_5)_4]$ and $[Cp^*Ir(dppm)H][B(C_6F_5)_4]$, as indicated by ^1H and ^{31}P NMR spectroscopy (see discussion).

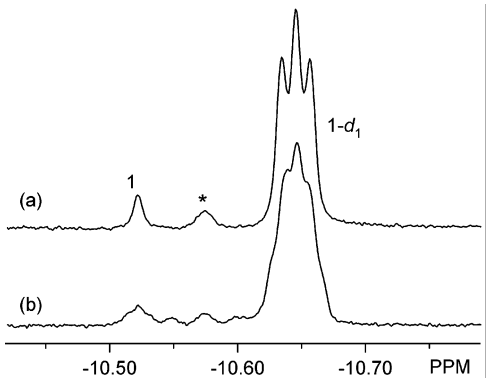

Figure 4. (a) Partial $^1H\{^{31}P\}$ NMR spectrum of $[Cp^*Ir(dmpm)HD]^{2+}$, **1**-d_1. (b) ^1H NMR spectrum (250 K, CD_2Cl_2, 750 MHz). The asterisk designates the resonance for the trans isomer.

4.2. T_1 and H−D Coupling in Complexes 1 and 2. Relaxation time determinations for the hydride resonances corresponding to the cis isomers of **1** and **2** were carried out using standard inversion recovery methods. For **2**, $T_{1(min)} = 157$ ms was measured at 255 K (750 MHz), while **1** gives $T_{1(min)} = 145$ ms at 240 K (500 MHz).

Complexes **1** and **2** do not incorporate deuterium in the hydride ligands when methylene chloride solutions were exposed to one atmosphere of D_2 gas for several weeks at 250 K or for several hours at room temperature. Partially deuterated samples were ultimately prepared by carrying out the synthetic procedure under one atmosphere of HD gas. A representative ^1H NMR spectrum of the hydride region of complex **1**-d_1 is shown in Figure 4.

Using $^1H\{^{31}P\}$spectra, measurement of J_{HD} values for **1**-d_1 and **2**-$d_1$was carried out at over a range of temperatures. In contrast to the previously reported Ru analogue of **2**, where J_{HD} values slightly decreased with temperature, the observed values of J_{HD} for **1** and **2** *increase* significantly when the observation temperature is increased (see Figure 5). For complex **2**, the HD coupling declines slightly at higher temperatures due to a slow exchange process with the trans isomer, which was confirmed by EXSY NMR spectroscopy.

These observations also allowed for evaluation of the isotope shift caused by deuteration, which is upfield for both **1** and **2**.

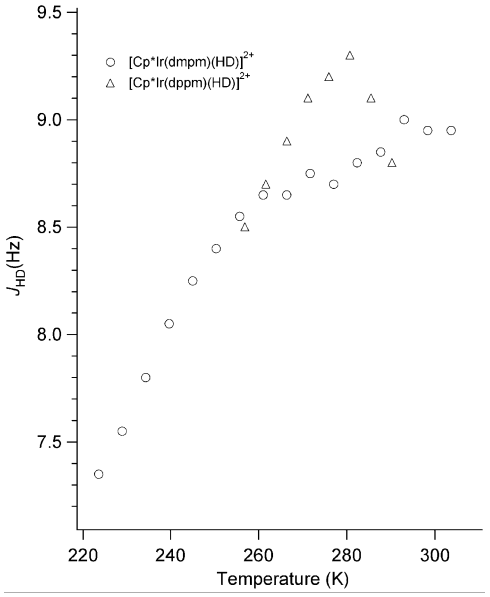

Figure 5. Plot of J_{HD} versus temperature for **1**-cis-d_1 and **2**-cis-d_1. Estimated uncertainties are ±0.3 Hz at low temperatures and ±0.2 Hz at higher temperatures.

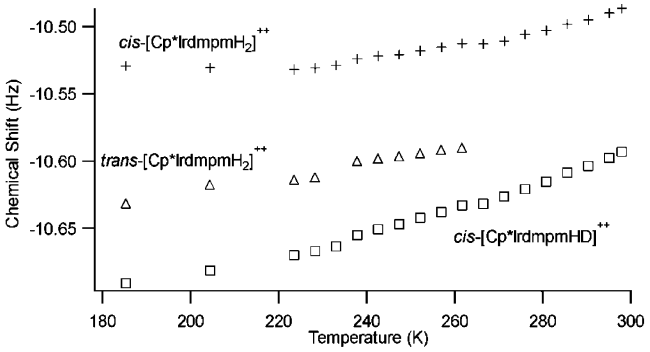

Figure 6. Chemical shifts as a function of temperature for the hydride resonances of **1** and **1**-d_1. The trans isomer shows no measurable isotope shift.

At 300 K, the resonance for **1**-d_1 is observed 100 ppb upfield of that for **1**. This difference increases slightly with decreasing temperature, reaching 134 ppb at 223 K (see Figure 6).

4.3. Theoretical Studies. The theoretical study consists of two parts: First, electronic structure calculations are performed to obtain an approximation to the potential energy (PE) surface of the complex. Second, nuclear dynamics calculations are carried out on this surface to obtain the vibrational energy levels and the coresponding wave functions.

For complex $\mathbf{1}^{2+}$, DFT calculations with the B3LYP functional have been used to determine electronic energies and wave functions. The nuclear dynamics calculations allow the determination of vibrational eigenstates connected to the motion of the hydrogen atoms. To this end, the matrix representation of the Hamiltonian operator for such motion was constructed by using the standard discrete variable representation (DVR) method, as implemented by Colbert and Miller.[19] Diagonalization of this matrix yielded vibrational energy levels and wave functions. The procedure followed to carry out the nuclear dynamics calculations is essentially a 1D version of the procedures previously reported.[4]

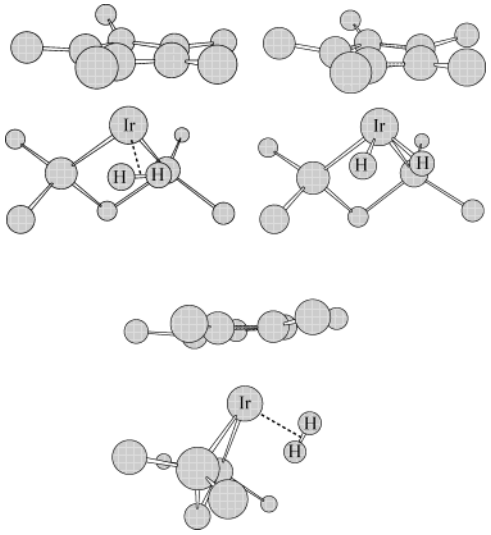

Figure 7. Optimized structures for the dihydrogen minimum (top left), dihydride minimum (top right), and librational transition structure (bottom). All hydrogen atoms except the dihydrogen ligand have been omitted. The point of view for the structure of the librational transition structure is different from the other two to highlight the orientation of the dihydrogen ligand.

Table 2. Geometries of the Stationary Points for Complex $\mathbf{1}^{2+}$ and Energies Relative to the Dihydride Minimum

structure	R_{HH} (Å)	R_{Ir-H2} (Å)	∠H–Ir–H (deg)	R_{Ir-P} (Å)	$R_{Ir-C(Cp)}$[a] (Å)	∠P–Ir–P (deg)	*E* (kcal/mol)
dihydrogen	0.93	1.65	31.7	2.40	2.30	71.4	1.4
dihydride	1.63	1.37	61.3	2.40	2.32	70.6	0.0
TS dihydrogen-dihydride	1.12	1.55	39.7	2.40	2.31	71.2	1.7
librational TS	0.84	1.73	26.9	2.41	2.30	71.6	6.3

[a] C(Cp) stands for the five carbon atoms forming the cyclopentadienyl ring.

Localization of the stationary points revealed that both dihydrogen and dihydride structures exist within C_s symmetry, all of them *cisoid*. The most stable structure found is the dihydride structure, with $R_{HH} = 1.63$ Å. Only 1.4 kcal/mol higher in energy is the dihydrogen structure, with $R_{HH} = 0.93$ Å. The transition state that connects both structures (with a unique imaginary frequency of 619*i* cm^{-1}) is only 1.7 kcal/mol higher in energy than the dihydride structure and, consequently, only 0.3 kcal/mol above the dihydrogen structure, a vanishingly small barrier. A second transition state structure for the librational motion of the H_2 ligand is 6.3 kcal/mol above the dihydride minimum, which indicates that a slow rotation regime of the H_2 unit can be assumed. It has been characterized as a transition structure with a unique imaginary frequency of 546*i* cm^{-1}. Representations of the structures of these stationary points are depicted in Figure 7. The transition state for the dihydrogen to dihydride isomerization is not shown, due to its similarity to the dihydrogen structure. Geometrical parameters and energies for these structures are tabulated in Table 2.

Nuclear dynamics calculations were undertaken using a one-dimensional PE surface or, more properly, a PE profile. A relaxed PE surface was derived by fixing the H−H distance at different values and allowing the complex to relax to a restricted minimum. Because all atoms have changed their positions from one point to the next, the PE profile is constructed using as"path" a collective variable *s*, whose value is determined by finding

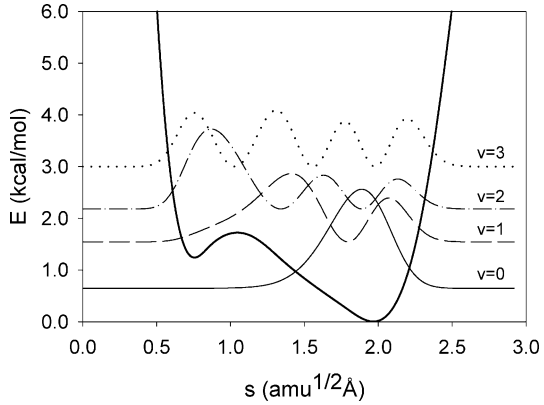

Figure 8. Relaxed potential energy profile for the elongation of the H−H distance, and probability density for the first vibrational states. The abscissa values correspond to distances in mass-weighted Cartesian coordinates.

Table 3. Vibrational Energy Levels and Geometrical Expectation Values of the R_{HH} Distance

state	E (kcal/mol)	$\langle s\rangle_i$ (amu$^{1/2}$ Å)	$\langle R_{HH}\rangle_i$ (Å)
0	0.65	1.85	1.54
1	1.55	1.51	1.37
2	2.18	1.23	1.19
3	3.00	1.45	1.34
4	4.07	1.48	1.36
5	5.27	1.51	1.37
6	6.58	1.54	1.39
7	7.97	1.58	1.40
8	9.42	1.61	1.42
9	10.91	1.65	1.44

the distance in mass-weighted Cartesian coordinates between pairs of consecutive points (more on this in the Discussion section). In this PE profile, the dihydrogen minimum is at $s = 0.76$ amu$^{1/2}$ Å, and the dihydride one is at $s = 1.96$ amu$^{1/2}$ Å. Figure 8 displays the relaxed PE profile as well as the probability density ($|\Psi_i|^2$) for the lowest vibrational states.

Building the DVR matrix representation of the nuclear motion Hamiltonian over the PE profile $U(s)$ and diagonalizing give a set of stationary states corresponding to vibrational energy levels and nuclear wave functions for a system confined to the monodimensional potential $U(s)$. Finally, from the vibrational wave functions, it is straightforward to derive expectation values for the collective coordinate s and obtain from it the corresponding H−H distances by reversing the fit used when computing the path variable s in the fitting of the PE profile. The expected geometry for each vibrational state i is determined by calculating the expectation value for the collective variable s using eq 2:

$$\langle s\rangle_i = \frac{\langle \Psi_i|\hat{s}|\Psi_i\rangle}{\langle \Psi_i|\Psi_i\rangle} \qquad (2)$$

In eq 2, Ψ_i is the wave function for the ith vibrational state. Expectation values for the HH distance, $\langle R_{HH}\rangle_i$, for each vibrational state are estimated by interpolation of the $\langle s\rangle_i$ values used in building the relaxed PE profile of Figure 8. The final results are gathered in Table 3. The expectation value of the HH distance determined for the ground state is 1.54 Å. The effect of temperature was estimated by computing the Boltzmann average of $\langle R_{HH}\rangle$. The mean HH distance decreases with temperature, as depicted in Figure 9.

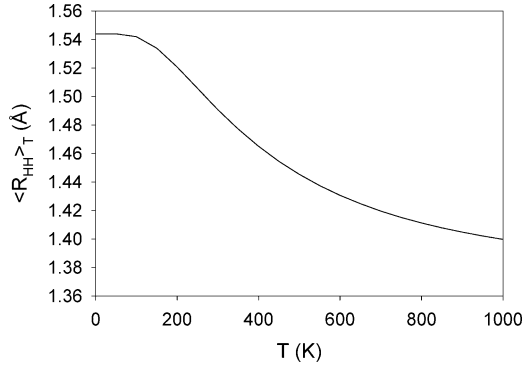

Figure 9. Calculated temperature dependence of the HH distance.

5. Discussion

5.1. Synthesis. The preparation of the cationic metal halide precursors follows closely the procedure reported by Valderrama[20] and co-workers, for the preparation of [Cp*Rh(dppm)Cl]Cl and [Cp*Ir(dppm)Cl]Cl. The previous procedure employs 2 equiv (per metal atom) of the appropriate bidentate phosphine to a methanol solution of $[Cp^*IrCl_2]_2$ or $[Cp^*RhCl_2]_2$. We have found that addition of 4 equiv of phosphine reduces the formation of byproducts and simplifies workup of the reaction mixture. The new complex, [Cp*Ir(dmpm)Cl]Cl, was conveniently prepared in 78% yield by this procedure.

The X-ray structure of the $B(C_6F_5)_4$ salt shows the expected geometry, with no unusual intermolecular contacts between the anion and the cation. The closest C···F distances are 3.048 Å and 3.219 Å for the Cp* and dmpm ligands, respectively. The Ir−Cl bond distance is 2.44 Å, comparable to the value 2.38 Å reported for the ruthenium analogue Cp*Ru(dmpm)Cl.[21] Since previous reports indicated that the Ru bound chloride was very labile, we were optimistic that halide abstraction reactions from the Rh and Ir centers would be feasible.

In contrast to the facile chloride displacement observed for Cp*Ru(dmpm)Cl, no reaction was observed when methylene chloride solutions of [Cp*Ir(dmpm)Cl]Cl were treated with $NaB(C_6F_5)_4$ under hydrogen gas. With $AgPF_6$ or $AgBF_4$ under hydrogen, reaction is rapid but leads to complex mixtures of intractable products. Seeking a highly reactive halide abstracting agent which can be combined with a noncoordinating anion, we found that the silyl cation $[Et_3Si][B(C_6F_5)_4]$ reported by Lambert and co-workers[22] gives efficient chloride abstraction from Rh and Ir chlorides. Complexes **1** and **2** and the new Rh complex $[Cp^*Rh(dmpm)(H_2)][B(C_6F_5)_4]_2$ were conveniently prepared by this method (see Scheme 1). The Rh complex is thermally labile, but the Ir complexes **1** and **2** are stable at room temperature. As expected for dicationic hydride complexes, these species are extremely acidic, being readily deprotonated by even traces of water. Typical of this reactivity is deprotonation of complex **1**, which affords $[Cp^*Ir(dmpm)(H)]^+$. An attempt to

(20) Valderrama, M.; Contreras, R.; Bascuñan, M.; Alegria, S. *Polyhedron* **1994**, *14* (15−16), 2239.
(21) Smith, D. C., Jr.; Haar, C. M.; Luo, L.; Li, C.; Cucullu, M. E.; Mahler, C. H.; Nolan, S. P.; Marshall, W. J.; Jones, N. L.; Fagan, P. J. O*rganometallics* **1999**, *18*, 2357.
(22) Lambert, J. B.; Zhang, S.; Ciro, S. M. *Organometallics* **1994**, *13*, 2430.

regenerate **1** by treatment of $[Cp^*Ir(dmpm)(H)]^+$ with triflic acid gave no reaction, consistent with the very high acidity of **1**.

5.2. Structure of the Rhodium Complex. Given the important role of Rh complexes in homogeneous hydrogenation, the relative scarcity of well documented dihydrogen complexes of rhodium is surprising.[23] Based on the observed J_{HD} value of 31 Hz, $[Cp^*Rh(dmpm)(H_2)][B(C_6F_5)_4]_2$ is formulated as a dihydrogen complex with a H−H distance of ca. 0.90 Å. The previously reported singly charged Ru analogue with the same ligand set has $J_{HD} = 17$ Hz, consistent with a H−H distance of 1.2 Å. Presumably, this large structural difference can be attributed to significantly greater back-donation from the electron-rich Ru center into the σ^* orbital of the bound H_2 ligand. The dicationic Rh center lacks sufficient electron density in metal d orbitals for efficient back-donation to the bound H_2. Ru dihydrogen complexes with comparable structures are known, but electron-withdrawing coligands are required, e.g., $[Cp^*Ru(CO)_2(H_2)]^+$, which has $J_{HD} = 28$ Hz.[24]

5.3. Structure of the Iridium Complexes. Complexes **1** and **2** exhibit two different hydride resonances, with quite different H−P couplings. Based on previous reports for cationic Ru and Os analogues, these can initially be assigned to cisoid and transoid isomers in a capped square pyramidal geometry. For complex **1**, the predominant *cisoid* isomer has $J_{HP} = 6$ Hz, while the minor *transoid* isomer exhibits $J_{HP} = 20$ Hz. This situation is similar to that reported by Jia and co-workers for the Os cation $[CpOs(dppm)H_2]^+$, where the *cisoid* isomer has $J_{HP} = 6.5$ Hz, while the *transoid* isomer has $J_{HP} = 31.8$ Hz.[25] The cis/trans ratio varies significantly, depending upon the identity of the phosphine ligand, with the more sterically demanding dppm ligand leading to a ratio of 65:35, while the more compact dmpm ligand gives a ratio of 97:3. This is readily explicable in terms of steric interactions between the phosphine ligand phenyl rings and the methyl groups of the Cp* ligand, which tend to favor the transoid geometry.

A useful method for characterization of dihydrogen complexes is the measurement of dipole−dipole relaxation rates in the ^{1}H NMR resonance for bound hydrogen. At the temperature where the maximum rate of relaxation is observed ($T_{1(min)}$), use of the methodology developed by Halpern and co-workers[26] allows the determination of the H−H distance in a dihydrogen or dihydride complex. For complexes **1** and **2**, the minimum relaxation times measured for the resonance due to the cisoid isomers are 219 ms for **1** and 155 ms for **2** (750 MHz). Assuming the slow rotation regime, the H−H distances derived by this method are 1.49 Å and 1.45 Å, respectively.

5.4. H−D Coupling in 1 and 2. H−D couplings were determined over a range of temperatures for samples of **1**-d_1 and **2**-d_1. Interestingly, the observed couplings *increase* significantly with increasing temperature, ranging for complex **1** from ca. 7.5 Hz at 220 K up to ca. 9 Hz at 300 K. This temperature dependence contrasts with the behavior previously reported for the singly charged Ru analogues, where a modest decrease in H−D couplings with temperature was observed for $[Cp^*Ru(dppm)(H_2)]^+$.

In an earlier communication on the properties of **1**,[9] it was noted that the J_{HD} value of 8.1 Hz observed at 240 K is consistent with a H−H distance of 1.34 Å, using the correlation between H−H distance and H−D coupling developed by Limbach and Chaudret.[8] This value is not consistent with the distance 1.49 Å determined from the relaxation data described above. This discrepancy has led us to a reexamination of the relationship between J_{HD} and H−H distance.

Early analysis of this correlation focused on the H−H distance range 0.8−1.2 Å, where abundant structural data from neutron diffraction and solid-state NMR studies are available.[6,7] This led to the development of a simple inverse linear relationship between J_{HD} and R_{HH}. Subsequently, Limbach and Chaudret reported a more sophisticated analysis based on application of the bond-valence bond-length concept to hydride and dihydrogen complexes.[8] To express J_{HD} as a function of R_{HH} or vice versa, they based their model on the relation derived by Hush, $^1J_{HD} = 43P_{HH}$.[27] A two-bond term was added to account for magnetic couplings in trans polyhydrides. This additional term is proportional to the square of P_{MH}, the metal hydrogen bond order. The distance $R°_{HH}$ is set to 0.74 Å. The constants b_{MH} and b_{HH} used by Limbach and Chaudret are decay parameters previously determined to be 0.404 Å in N−H···H hydrogen bonded systems. The M−H distance $R°_{MH}$ was set to 1.6 Å.[8] The following expression was obtained, where $J_{LL'}$ is the magnetic coupling between L and L′ and γ (L) is the gyromagnetic ratio of L (L, L′ = H, D, T):

$$J_{LL'} = J_{HH}\gamma(L)\gamma(L')/\gamma(H)^2 = {}^1J_{LL'}°P_{HH} + {}^2J_{LL'}°(1 - P_{HH})^2$$

or

$${}^1J_{HD} = (43 - 2^2\,J_{HD})\exp\left[\frac{0.74 - R_{HH}}{b}\right] + {}^2J_{HD}\left\{\exp\left[\frac{0.74 - R_{HH}}{b}\right]\right\}^2 + {}^2J_{HD} \quad (3)$$

Assuming $b = 0.404$ and $^2J_{HD} = -2.8$ Hz, eq 3 can be rearranged and simplified to become

$$R_{HH} = 0.74 - 0.404\ln\{0.5(17.3571 - [301.27 - 4(1 + 0.351\,43\,J_{HD})]^{0.5})\}(Å) \quad (4)$$

In the model of Limbach and Chaudret, the decay parameter b and the two-bond coupling $^2J_{HD}$ are fixed to 0.404 Å and −2.8 Hz, respectively. These values are based on previous work and experimental data available. To verify this model, Limbach and Chaudret tabulated H−H and M−H distance data for a variety of dihydrogen and polyhydride complexes determined by neutron and X-ray diffraction and plotted them against the

(23) Several Rh polyhydride complexes which include a dihydrogen ligand are known. For example, $[Cp^*Rh(PMe_3)(H_2)H]^+$ (Taw, F. L.; Mellows, H.; White, P. S.; Hollander, F. J.; Bergman, R. G.; Brookhart, M.; Heinekey, D. M. *J. Am. Chem. Soc.* **2002**, *124*, 5100) and $Tp'Rh(H_2)H_2$ (Bucher, U. E.; Lengweiler, T.; Nanz, D.; von Philipsborn, W.; Venanzi, L. M. *Angew. Chem., Int. Ed. Engl.* **1990**, *29*, 548. Gelabert, R.; Moreno, M.; Lluch, J. M.; Lledós, A. *Organometallics* **1997**, *16*, 3805). The only well documented Rh complex reported to date with a single dihydrogen ligand is (PCP)Rh-(H_2), for which $J_{HD} = 33$ Hz has been reported: Xu, W.-W.; Rosini, G. P.; Gupta, M.; Jensen, C. M.; Kaska, W. C.; Krogh-Jespersen, K.; Goldman, A. S. *J. Chem. Soc., Chem. Commun.* **1997**, 2273.

(24) Chinn, M. S.; Heinekey, D. M.; Payne, N. G.; Sofield, C. D. *Organometallics* **1989**, *8*, 1824.

(25) Jia, G.; Ng, W. S.; Yao, J.; Lau, C.-P.; Chen, Y. *Organometallics* **1996**, *15*, 5039.

(26) Desrosiers, P. J.; Cai, L.; Lin, Z.; Richards, R.; Halpern, J. *J. Am. Chem. Soc.* **1991**, *113*, 4173. Some confusion about the units employed in the equations describing dipole−dipole relaxation has been recently clarified: Bayse, C. A.; Luck, R. L.; Schelter, E. J. *Inorg. Chem.* **2001**, *40*, 3463.

(27) Hush, N. S. *J. Am. Chem. Soc.* **1997**, *119*, 1717.

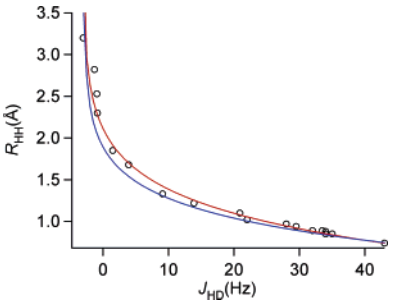

Figure 10. R_{HH} as a function of J_{HD}. The data used in the fittings are those published in ref 8. The blue line represents the relationship reported by Limbach and Chaudret (ref 8). The red line is derived using parameters discussed in the text.

values of J_{HD} reported for these complexes. As shown in Figure 10 (blue line), a reasonable fit of these data to eq 3 results. A significantly better correlation results from fitting the data with b and $^2J_{HD}$ defined as variable parameters. A least-squares fit against the experimental data allowed us to obtain the values of 0.494 Å for b and −3.04 Hz for $^2J_{HD}$. The plot of the resulting relation is shown as the red line in Figure 10.

Using this modified relationship between J_{HD} and R_{HH}, the observed value of J_{HD} for complex **1** of 8.1 Hz at 240 K corresponds to $R_{HH} = 1.45$ Å, which is in good agreement with the value determined from $T_{1(min)}$ at this temperature of 1.49 Å.

5.5. Temperature Dependence of H−H Bond Distances in Complexes 1 and 2. The observed values of J_{HD} increase significantly with increasing temperature, suggesting that the H−H bond distances in these complexes are *decreasing* with increasing temperature, in contrast to the situation with the cationic Ru analogue of **2**, where a small increase in HH distance was observed at higher temperatures. The observed couplings are independent of the magnetic field employed, which rules out the possibility that residual dipolar coupling could be responsible for the temperature dependence of the coupling.[28] In an earlier report, some of us had suggested that the observations for the iridium complex were qualitatively consistent with a dihydrogen/*cis*-dihydride equilibrium, with two distinct structures of similar energy in rapid equilibrium.[9] Attempts to quantitatively model this equilibrium using two limiting structures and reasonable estimates for the limiting couplings were not successful.[9] To resolve this problem, we have turned to combined quantum dynamics + density functional theory theoretical calculations.

5.6. Theoretical Studies. In contrast to the singly charged Ru analogues where a dihydrogen complex was the sole minimum, the calculated structures for stationary points in complex $\mathbf{1}^{2+}$ suggest that a dihydride structure with $R_{HH} = 1.63$ Å is slightly lower in energy than the dihydrogen structure with $R_{HH} = 0.93$ Å (see Table 2 and Figure 7). The very small calculated value of the energy barrier connecting the dihydrogen and dihydride minima makes it unlikely that either minimum corresponds to a separate chemical entity with real existence, for including vibrational zero-point energy could wash out the barrier (see Figure 8). Neither minimum correctly describes the structure found experimentally. Nonetheless, based on electronic structure results alone, one could conclude that complex **1** from a theoretical point of view is a dihydride complex, this being the most stable structure. This conclusion would be in agreement with the relative oxidative power of iridium and ruthenium: because ruthenium is more difficult to oxidize, $[Cp^*Ru(dppm)(H_2)]^+$ has a more stable dihydrogen minimum whereas complex **1** has a more stable dihydride minimum. One has to be cautious with this interpretation, however, because it is only accurate as far as the location of the minima on the potential energy hypersurface itself is concerned. The structure of a substance as determined from experiment is not necessarily related on a one-to-one basis with a given minimum in the potential energy hypersurface, because nuclear motion (which occurs even at 0 K) is missing from the latter. As far as nuclei are concerned, it is only a static picture. This situation is similar to what was encountered in the other elongated dihydrogen complexes studied before and even in apparently very different systems such as the so-called "low-barrier hydrogen bonds":[29] the fact that the "relevant" portion of the potential energy surface is very flat and anharmonic and that inclusion of vibrational motion (through consideration of the zero-point energy) is a must to account for the geometry of the complex. Complex $\mathbf{1}^{2+}$ differs from the other elongated dihydrogen complexes for which nuclear dynamics calculations have been done in that there is an actual potential energy barrier involved.

The motion of the light nuclei can be approximately accounted for by computing the full potential energy hypersurface $U(\mathbf{R})$, where $\mathbf{R}$ is a $3N$-6 dimensional vector of internal coordinates describing a given arrangement of the nuclei. This is difficult because of the high dimensionality, and some modeling is needed to reduce the dimensionality of the system. The simplest approach is to reduce the dimensionality of $U(\mathbf{R})$ to just one (monodimensional treatment). Generation of an acceptable monodimensional approximation to the full hypersurface that retains the key features of the problem is crucial here. This is in essence the process of building up a reduced potential energy surface depending on just one dynamical variable, the latter corresponding to some geometrical parameter of the complex (one of the components of $\mathbf{R}$ or a function of these).

A natural choice seems to be R_{HH} itself, for our interest lies in the dynamics of the H−H bond. This would mean constructing a potential energy profile by picking different geometries of the complex corresponding to different values of R_{HH} and computing the potential energy of these structures. A problem arises in this process when selecting the values of the rest of the geometric parameters of the complex, in particular, the Ir−H_2 distance. As can be seen in Table 2, the value of this parameter changes noticeably in the set of stationary points dynamically relevant (1.37 Å in the dihydride minimum, 1.65 Å in the dihydrogen minimum), so any "arbitrary" choice will be incorrect. Besides, in the previous elongated dihydrogen complexes studied, it was discovered that the dynamics of the H−H and M−H_2 bonds are inextricably intertwined.[30]

A solution exists that manages to combine both motions in a single dynamical variable: constructing a kind of "minimum energy path" coordinate. In this simplified representation, the potential energy profile is built with the energy of those points obtained by constraining R_{HH} to a set of values to span the

(28) Luther, T. A.; Heinekey, D. M. *J. Am. Chem. Soc.* **1997**, *119*, 6688.

(29) Garcia-Viloca, M.; Gelabert, R.; González-Lafont, A.; Moreno, M.; Lluch, J. M. *J. Am. Chem. Soc.* **1998**, *120*, 10203.

(30) Gelabert, R.; Moreno, M.; Lluch, J. M.; Lledós, A. *Chem. Phys.* **1999**, *241*, 155.

complete range of structures from dihydride to dihydrogen and then to optimize the resulting structures subject to this constraint on R_{HH}. The potential energy profile would, in this way, be relaxed with respect to all variables except R_{HH}, visit all relevant stationary points found, and represent in an appropriate way those areas of the potential energy surface in which the $Ir-H_2$ distance follows R_{HH} adiabatically.

One cannot use this relaxed potential energy profile as a function of R_{HH} directly in the dynamical calculations: the reason is that, by optimizing the complete complex at each point, any two points in this profile differ not only by the increment in H−H distance but also in the positions of the rest of nuclei. Therefore, the value of the mass in the kinetic operator in the nuclear Schrödinger equation is unclear. The solution to this problem is to define a new dynamical variable *s*, which corresponds to the path length along this potential energy profile in mass-weighted Cartesian coordinates. In this way, the mass is implicitly included in the kinetic energy operator, and the dynamical equations can be solved without any ambiguity in terms of *s*. To translate the relaxed potential energy profile from R_{HH} to *s*, one must orient all the optimized structures in the same way, order them from smallest to largest R_{HH} value, and then compute the length of the linear vector in mass-weighted coordinates that links any two consecutive structures in the complete configurational space. We think that this proposal is a reasonable option to capture, within the intrinsic limitations of a monodimensional treatment, the dynamical features arising from the motion of the light dihydrogen ligand.

The potential energy profile built in this way, because of the reasons explained above, can be appropriately called a "relaxed potential energy profile". Figure 8 displays the relaxed PE profile. The path length *s* is measured from an arbitrarily chosen point, picked to be a clear dihydrogen structure sufficiently high in energy (in particular, $R_{HH} = 0.50$ Å, which has $R_{Ir-H2} = 1.41$ Å, and whose energy is 60.6 kcal/mol above the dihydride minimum). In this profile, the dihydrogen minimum is at $s = 0.76$ amu$^{1/2}$ Å, and the dihydride minimum appears at $s = 1.96$ amu$^{1/2}$ Å.

As described in the Results section, diagonalization of the DVR matrix representation of the nuclear motion Hamiltonian over the PE profile $U(s)$ gives a set of stationary states corresponding to vibrational energy levels and nuclear wave functions for a system confined to the monodimensional potential $U(s)$. Expectation values for the collective coordinate *s* were derived from these, and the corresponding H−H distances were obtained by reversing the fit used when computing the path variable *s* in the fitting of the PE profile. Hence, we expect that a low-temperature neutron diffraction experiment will show a single structure with $R_{HH} = 1.54$ Å (see Table 3), even though with a certain width or uncertainty, as described by the probability density for the vibrational state $\upsilon = 0$ in Figure 8.

Some comments are warranted on the effects brought about by this monodimensional model. As explained, the path *s* is actually a kind of "minimum energy path" approach to the full $3N$-6 dimensional potential energy hypersurface that captures the relevant features for the dynamics of the dihydrogen ligand. However, one might wonder whether there is any flaw in this model that might affect the results and conclusions. Actually, the path being a monodimensional relaxed path, it crosses the dynamically relevant area of the potential energy hypersurface through areas with small curvature (or, in other words, of low frequencies). This has a bearing on the zero-point energy estimated, which mainly comes from the lowest frequency modes, so it is underestimated. If other relevant degrees of freeedom were included, zero-point energy would be increased, and if the shape of the potential energy profile is taken into account, the expectation values $\langle R_{HH}\rangle_i$ would likely change slightly.

The unusual shape of the PE profile, with a lower minimum in the dihydride region and a secondary shallow minimum in the dihydrogen region, has a bearing on the expectation values of the R_{HH} distance in vibrational excited states. In effect, the first few states display decreasing $\langle R_{HH}\rangle$ as the energy of the state increases, leading to a decrease in the mean H−H distance as temperature increases, as seen experimentally. The mean H−H distance measured at a certain temperature can be estimated by computing the Boltzmann average of $\langle R_{HH}\rangle$. The results are depicted in Figure 9, where the mean H−H distance decreases with temperature, in good agreement with experiment. The R_{HH} of 1.49 Å derived from $T_{1(min)}$ at 240 K can only be truly compared with mean values coming from a Boltzmann average at this temperature. Figure 9 shows that $\langle R_{HH}\rangle$ at $T \approx 250$ K is approximately 1.50 Å, in good agreement with experimental data.

The very small calculated value of the energy barrier connecting the dihydrogen and dihydride minima makes it unlikely that either minima corresponds to a separate chemical entity with real existence, for including vibrational zero-point energy could wash out the barrier. Neither minimum correctly describes the structure found experimentally. Contrary to the cases of the ruthenium complexes, in this case the most stable minimum is that of the dihydride structure, and the delocalization of the ground vibrational state pushes the expectation value toward shorter values of the H−H distance. Accordingly, this is a rather extreme case of an elongated dihydrogen complex, and a term like "compressed dihydride" may be a more appropriate descriptor for complexes of this type. Being aware of the limitations of theoretical calculations, we think that the description we propose here is reasonable and explains the available experimental results.

6. Summary and Conclusions

The previously reported discrepancy between R_{HH} values for **1** determined by relaxation and J_{HD} methods has been clarified by the development of an improved correlation between R_{HH} and J_{HD}. Good agreement is found between these experimental results and the results derived from quantum nuclear dynamics on a DFT potential energy profile, which also provide an explanation for the novel temperature dependence of the HH distance. Our results suggest that complexes such as **1** and **2** cannot be described adequately by a single *structure*, in the sense of the word usually used by chemists. Further, terms such as "elongated dihydrogen" or "compressed dihydride" should be used with caution. We favor the latter for **1** and **2** because the lowest minimum is actually a dihydride, with the caveat that the PE surface is extremely flat and the hydrogen atoms are extensively delocalized.

The complexes reported here allow us to evaluate the interactions of H_2 with a family of metal fragments of the form $[CpM(PP)]^{n+}$. As previously reported for Ru and Os ($n = 1$),

dihydrogen complexes (Ru) or cis dihydride complexes (Os) are observed. This is consistent with the general observation that the second row transition element prefers to form dihydrogen complexes and maintain a lower formal oxidation state than that of the corresponding third row element. In both cases, variable amounts of a trans dihydride isomer are observed, depending upon the steric and electronic contributions of the chelating phosphine ligand PP. In the Ru family, a wide range of HH distances are observed, depending upon the coligands. As previously reported, certain ligand combinations leading to HH distances of ca. 1.1 Å give novel temperature-dependent values of R_{HH}, due to the very soft PES corresponding to motion of the H atoms.

For the dicationic species ($n = 2$), we find that Rh gives a conventional dihydrogen complex with a short HH distance of *ca.* 0.9 Å. In contrast to Ru, no trans dihydride isomer is observed. This effect of charge in this case is analogous to the early observations on Re cations versus neutral W complexes, where $[(PCy_3)_2Re(CO)_3(H_2)]^+$ is entirely a dihydrogen complex, while the neutral tungsten analogue $(PCy_3)_2W(CO)_3(H_2)$ is in equilibrium with *ca.* 20% of a W^{II} dihydride complex.[31] Iridium complexes **1** and **2** are best described as compressed dihydride complexes with HH distances of about 1.5 Å. In the case of Ir, variable amounts of a trans dihydride isomer are also observed.

Acknowledgment. RG gratefully acknowledges the Ministerio de Ciencia y Tecnología of Spain for a Ramón y Cajal research contract. This research was supported by the Spanish Ministerio de Ciencia y Tecnología under Projects BQU2002-00301 and BQU-2002-04110-C02-02. D.M.H. is grateful to the U.S. National Science Foundation for support of this research. Acquisition of the 750 MHz NMR spectrometer was supported by the National Science Foundation and the Murdoch Charitable Trust.

Supporting Information Available: Details of the X-ray structure determination for $[Cp^*Ir(dmpm)Cl][B(C_6F_5)_4]$. This material is available free of charge via the Internet at http://pubs.acs.org.

JA048775L

(31) Heinekey, D. M.; Radzewich, C. E.; Voges, M. H.; Schomber, B. H. *J. Am. Chem. Soc.* **1997**, *119*, 4172.